Compact pairwise models for epidemics with multiple infectious stages on degree heterogeneous and clustered networks

Article (Accepted Version)

Compact pairwise models for epidemics with multiple infectious stages on degree heterogeneous and clustered networks

N. Sherborne, K.B. Blyuss*, I.Z. Kiss

Department of Mathematics, University of Sussex, Falmer,
Brighton, BN1 9QH, United Kingdom

August 31, 2016

Abstract

This paper presents a compact pairwise model that describes the spread of multi-stage epidemics on networks. The multi-stage model corresponds to a gamma-distributed infectious period which interpolates between the classical Markovian models with exponentially distributed infectious period and epidemics with a constant infectious period. We show how the compact approach leads to a system of equations whose size is independent of the range of node degrees, thus significantly reducing the complexity of the model. Network clustering is incorporated into the model to provide a more accurate representation of realistic contact networks, and the accuracy of proposed closures is analysed for different levels of clustering and number of infection stages. Our results support recent findings that standard closure techniques are likely to perform better when the infectious period is constant.

1 Introduction

Mathematical models of infectious diseases have proven to be an invaluable tool in understanding how diseases invade and spread within a population, and how best to control them [1, 2, 3]. Given a good understanding of the biology of the disease and of the behaviour and interaction of hosts, it is possible to develop accurate models with good predictive power, which provide the means to develop, test and deploy control measures to mitigate the negative impacts of infectious diseases, a good example being influenza [4]. However, as has been highlighted by the recent Ebola outbreak in West Africa [5], models can be very situation-specific and can become highly sophisticated or complex depending on intricacies of the structure of the population and the characteristics of the disease.

In the last few decades the use of networks to describe interactions between individuals has been an important step change in modelling and studying disease transmission [6, 7, 8, 3]. There is now overwhelming empirical evidence that in many practical instances individuals interact in a structured and selective way, e.g. in the case of sexually transmitted diseases [9]. Thus, the well-mixed assumption of early compartmental models [10] has to be relaxed or models need to be refined by including multiple classes and mixing between classes. However, in some cases a network representation could be more realistic than a description based on compartmental models. Conventionally, nodes in network-based models represent individuals, and the edges describe connections

*Corresponding author. Email: k.blyuss@sussex.ac.uk

between people who have sufficient contact to be able to transmit the disease [8, 7, 3]. This study focuses on static undirected networks, in which the edges of the network do not change over time, and all connections are sufficient to transmit the disease in either direction. The total number of edges a node has is known as its degree, and the frequency of nodes with different degrees is determined by a specific *degree distribution* $P(k)$ which can either be empirically measured or given theoretically. In either case $P(k)$ is the probability of a randomly chosen node having degree k. Early network models often assumed regular networks where all nodes have the same degree, or well-studied networks from graph theory, such as the Erdős-Rényi random graphs [11]. However, empirical research showed that real biological, social or technological networks do not conform to such idealised models. In fact, many studies on human interactions ranging from sexual contact networks [9] to using the travel of banknotes as an indicator of human activity [12], or even internet connectivity [13] have observed *wide-tail distributions*, with the majority of nodes having a low number of contacts, and a few nodes in the network having a much higher degree. This structure is most closely approximated by scale-free networks described by a power-law degree distribution $P(k) \sim k^{-\alpha}$ with some positive exponent α, which for most accurately described human contact patterns lies in the range $\alpha \in [2, 3]$ (see, for example, [14]). The impact of contact heterogeneity on the spread of epidemics is significant, and studies have highlighted the disproportionate role which may be played by a few highly-connected nodes [15].

Another striking feature of real social contact patterns is the presence of small and highly-interconnected groups which occur much more frequently than if edges were to be distributed at random. This is known as *clustering*, and its presence in empirical data [16, 17] has driven the need to consider network models that include this feature. Perhaps, one of the most well-known and parsimonious theoretical models with tuneable clustering is the small-world network [18], where nodes are placed on a ring, and the network is dominated by local links to nearest neighbours with a few links rewired at random, which means that the average path length is not too large and comparable to that found in equivalent random networks. For a summary of numerous alternative algorithms that can be used to generate clustered networks see, for example, [19] or [20]. It is well known that modelling epidemic spread on such networks is more challenging, although some models have successfully incorporated clusterings [21, 22, 23, 24, and references therein]. However, it is often the case that such models only work for networks where clustering is introduced in a very specific way, e.g. by considering non-overlapping triangles or other subgraphs of more than three nodes.

Besides the details of the network structure, another major assumption that significantly reduces the mathematical complexity of models and makes them amenable to analysis with mean-field models of ordinary differential equations and tools from Markov chain theory is the assumption that the spreading/transmission of infection and recovery processes are Markovian. However, it has long been recognised that this is often not the case, and, for example, the infectious periods are typically far from exponential, and, perhaps, are better described by a normal-like or peaked distribution [25, 26, 27]. Modelling non-Markovian processes can be challenging and often leads to delay differential or integro-differential equations that are much more difficult to analyse. Recently, [28] have put forward a generalisation of a pairwise model for Markovian transmission with a constant infectious period for a susceptible-infected-recovered (SIR) dynamics, with a further recent extension by the same authors to an arbitrary distribution of the recovery time [29]. The first generalisation resulted in a model given by a system of delay differential equations with discrete and distributed delays which makes it possible to gain insight into how the non-Markovian nature of the recovery process affects the epidemic threshold and the final epidemic size. Other important recent research in this direction includes the message passing formalism [30, 31] and an approach based on renewal theory [32].

In light of the importance of the above-mentioned network properties (i.e. degree heterogeneity and clustering) and the non-Markovian nature of the spreading and/or recovery processes, in this paper we generalise our recent research on a multi-stage SIR epidemics [33] and focus on modelling a Markovian spreading process with gamma-distributed infectious period on networks that account for heterogeneous degree distribution and clustering. This is achieved within the framework of pairwise models [6], and we show that the additional model complexity induced by degree heterogeneity and non-Markovian recovery can be effectively controlled via a reduction procedure proposed by [34]. This allows one to derive an approximate deterministic model that helps numerically determine the time evolution of the epidemic and the final epidemic size. Moreover, the model allows us to gain insights into the interactions of the three main model ingredients, namely, degree heterogeneity, clustering and non-exponential recovery and the agreement between the model and the stochastic network simulation. The paper is organised as follows. In the next section we derive a compact pairwise model for unclustered networks whose size is independent of the range of degrees and derive and discuss some analytical results for this model. All results are validated by comparing the numerical solution of the pairwise model to results from direct stochastic network simulation. In Section 3, we investigate the case when the same epidemic unfolds on clustered networks. The corresponding pairwise model is derived, and we discuss the extra complexities necessary to more accurately approximate the spread of the disease. More importantly, we investigate how clustering and the non-Markovian recovery affect the agreement between the pairwise model and simulations. Finally, in Section 4 we conclude with a discussion of our results and future work.

2 Disease dynamics in the absence of clustering

As a first step in the analysis of the spread of epidemics on unclustered networks, we introduce the necessary concepts from multi-stage infections and pairwise models [33]. In the SI^KR model, once a susceptible individual S becomes infected, they progress through K equally infectious stages denoted as $I^{(i)}$, $1 \leq i \leq K$. The transition rates between successive stages are given by $K\gamma$. Thus, in simulation the times spent in each of the K stages are independent exponentially distributed random numbers. The total time of infection is, therefore, the sum of K exponential distributions, which is a gamma distribution with the mean time of γ^{-1} [35]. In order to describe the dynamics of an epidemic we consider the state of the nodes in the network and the edges connecting them. Since a susceptible individual can only become infected upon a transmission across an $S - I^{(i)}$ link we need to consider the expected number of edges connecting susceptible and infected individuals in any stage i from 1 to K at time t over the whole network, to be denoted as $[SI^{(i)}](t)$. Here we have taken $[SI^{(i)}]$ independently of the degrees of the nodes in state S and $I^{(i)}$, i.e. $[SI^{(i)}] = \sum_{a,b}[S_a I_b^{(i)}]$ where a and b denote the degrees in the range between the minimum and maximum degrees in the network, denoted as k_{min} and k_{max}, respectively. This definition applies to all pairs, i.e. $[AB]$ stands for the population level count of all $A-B$ edges taken across all possible connections between nodes of different degrees;

$$[AB] = \sum_{a,b}[A_a B_b], \quad \text{and} \quad A, B \in \{S, I^{(1)}, I^{(2)}, \ldots, I^{(K)}, R\} := \mathbb{S}.$$

Here and henceforth $\mathbb{S}$ will denote the set of all possible states for a node. The expected number of $S - S$ edges depends on the expected number of $S - S - I^{(i)}$ triples, with this being the case for other edge types as well. To break the dependency on higher order moments, closure relations must be introduced which allow us to approximate the number of triples using the number of pairs and nodes in different states [6].

We begin our analysis by considering the simpler case where the contact network has a locally tree-like structure characterised by zero clustering. The Markovian, or single stage, approach can be extended to a SI^KR multi-stage model. In order to obtain a pairwise model for the SI^KR dynamics for unclustered and degree heterogeneous networks, we start with the unclosed model for a general K-stage disease and describe an *a priori* method to derive a new set of closures at the level of triples. It should be noted that our approach resembles that used in recent works of [34] and [36]. The system describing the dynamics of a K-stage disease has the following form [33]

$$\begin{aligned}
&[\dot{S}] = -\tau[SI],\\
&[\dot{I^{(1)}}] = \tau[SI] - K\gamma[I^{(1)}],\\
&[\dot{I^{(j)}}] = K\gamma[I^{(j-1)}] - K\gamma[I^{(j)}], \quad \text{for} \quad j = 2, 3, \ldots, K,\\
&[\dot{SS}] = -2\tau[SSI],\\
&[\dot{SI^{(1)}}] = -(\tau + K\gamma)[SI^{(1)}] + \tau\left([SSI] - [ISI^{(1)}]\right),\\
&[\dot{SI^{(j)}}] = -(\tau + K\gamma)[SI^{(j)}] + K\gamma[SI^{(j-1)}] - \tau[ISI^{(j)}], \quad \text{for} \quad j = 2, 3, \ldots, K,\\
&[\dot{SR}] = -\tau[ISR] + K\gamma[SI^{(K)}],
\end{aligned} \tag{1}$$

where τ is the per-link disease transmission rate, and the terms without superscripts represent summation over all infected compartments, i.e. $[SI] = \sum_{i=1}^{K}[SI^{(i)}]$, $[SSI] = \sum_{i=1}^{K}[SSI^{(i)}]$ and $[ISI^{(j)}] = \sum_{i=1}^{K}[I^{(i)}SI^{(j)}]$. While the above equations do not seem to account separately for the degrees of the nodes, we will show that it is possible to keep such a system and include all the information about the degree distribution in a new closure relation at the level of pairs. The closure for this model can be obtained by first considering the classical triple closure for a regular network [37]

$$[XSI^{(i)}] \approx \frac{n-1}{n}\frac{[XS][SI^{(i)}]}{[S]}, \tag{2}$$

where n is the degree of every node in the network (and thus also the mean degree), and $X \in \mathbb{S}$. The derivation of a new closure for heterogeneous networks starts from noting that closure (2) depends on the degree of the middle node, which allows us to write

$$[XS_aY] \approx \frac{a-1}{a}\frac{[XS_a][S_aY]}{[S_a]}, \quad X, Y \in \mathbb{S}, \tag{3}$$

for a susceptible node of degree a, with $a \in [k_{min}, k_{max}]$. To make further progress, one can use the approximation used by [38],

$$[S_aY] \approx [SY]\frac{a[S_a]}{\sum_{b=k_{min}}^{k_{max}} b[S_b]}. \tag{4}$$

This assumes that the number of $S_a - Y$ pairs is approximately equal to the number of $S - Y$ pairs (regardless of node degree) multiplied by the degree-biased fraction of S nodes with degree a. Substituting this approximation into (3) yields

$$[XS_aY] \approx [XS][SY]\frac{a(a-1)[S_a]}{T_1^2}, \tag{5}$$

where

$$T_1 := \sum_{b=k_{min}}^{k_{max}} b[S_b] = [SS] + \sum_{i=1}^{K}[SI^{(i)}] + [SR]$$

denotes the total number of edges emanating from susceptible nodes. The second expression for T_1 above follows directly from the pairwise model (1) and explains the need for explicitly including an equation for $[SR]$. Taking the sum of all triples in (5) over all degrees a gives

$$[XSY] = \sum_{a=k_{min}}^{k_{max}} [XS_aY] \approx [XS][SY]\frac{T_2 - T_1}{T_1^2}, \tag{6}$$

with

$$T_2 = \sum_{b=k_{min}}^{k_{max}} b^2[S_b].$$

Unfortunately, T_2 cannot be expressed in a closed form from the solution of system (1). However, it should be possible to estimate the degree distribution of susceptible nodes [39, 34]. This distribution is given by

$$s_k := [S_k]/[S],$$

and has the mean

$$n_S = T_1/[S].$$

[34] have shown by means of numerical simulation that the (dynamic) degree distribution of susceptible nodes is proportional to the degree distribution $P(k)$ for a Markovian SIS epidemic. A similar approach is applied below in the context of SI^KR dynamics under the assumption that a similar level of accuracy can be obtained (see Discussion for numerical arguments supporting this assumption). This linear relationship between s_k and $P(k)$ in then used to derive a compact model. A brief explanation is given below, and the full details of the method can be found in [34]. As they will be needed later, we first introduce the moments of the degree distribution $P(k)$, namely,

$$n_i = \frac{\sum_{m=k_{min}}^{k_{max}} m^i N_m}{N} = \sum_{m=k_{min}}^{k_{max}} m^i P(m).$$

It is easy to see that

$$T_2 = [S] \sum_{m=k_{min}}^{k_{max}} m^2 s_m,$$

and so our goal is to find an estimate for s_k. Introducing a new variable $q_k = s_k/P(k)$ linearity enforces the following relation for all $k \in [k_{min}, k_{max}]$

$$\frac{q_k - q_{k_{min}}}{k - k_{min}} = \frac{q_{k_{max}} - q_{k_{min}}}{k_{max} - k_{min}}.$$

By manipulating this equation one can identify a relation between s_k and $P(k)$; namely

$$s_k = \frac{(k - k_{min})\, q_{k_{max}} + (k_{max} - k)\, q_{k_{min}}}{k_{max} - k_{min}} P(k). \tag{7}$$

Since the sum of all s_k's is one, and the distribution has the mean n_S, it is then possible to recast $q_{k_{min}}$ and $q_{k_{max}}$ in terms of the known quantities n_1, n_2, n_3 and n_S. Feeding these back into (7) gives an estimate for s_k, and thus T_2. Using this estimate we arrive at the following relation

$$\frac{T_2 - T_1}{T_1^2} \approx \frac{1}{n_S^2[S]} \left(\frac{n_2(n_2 - n_1 n_S) + n_3(n_S - n_1)}{n_2 - n_1^2} - n_S \right).$$

This gives the closure for the heterogeneous compact pairwise SI^KR model (1) in the form

$$[XSY] \approx \zeta(t)\frac{[XS][SY]}{[S]}, \tag{8}$$

where

$$\zeta(t) = \frac{n_2(n_2 - n_1 n_S) + n_3(n_S - n_1)}{n_S^2\left(n_2 - n_1^2\right)} - \frac{1}{n_S}. \tag{9}$$

It is evident that the range of degrees and the degree distribution have been implicitly accounted for in the closure relation, thus allowing us to work with a set of equations whose size is independent of the range of degrees. In other words, regardless of the exact nature of the contact network we will only ever need $2K+3$ equations in (1) to model the epidemic. This is due to all of the information about the degree distribution being included in $\zeta(t)$. In the special case of regular contact networks, where every node has the same degree n, one has that $n_S = n_1 = n$, $n_2 = n^2$ and $n_3 = n^3$, hence $\zeta(t)$ reduces to

$$\zeta = \frac{n-1}{n},$$

and the closure reverts back to the simpler version given in (2).

2.1 Numerical simulation results

In order to test the effectiveness of model 1) with closure (8), we compare its output to numerical simulation of epidemics spreading on networks with bimodal and truncated scale-free degree distributions, with both types of networks being constructed using the configuration model [40]. In the case of networks with a bimodal degree distribution, a chosen proportion of nodes are given k_1 half-edges, whilst the remainder are given k_2 half-edges, and these are then connected at random to construct the network. The generation of truncated scale-free networks begins by choosing bounds of minimum and maximum degree k_{min} and k_{max}. One then generates a power law distribution with a chosen exponent α and samples the normalized probability of a node having degree $k \in [k_{min}, k_{max}]$, after which half-edges are drawn and connected at random. If the total number of half-edges is odd, one is removed at random, the effect of which is small and diminishes rapidly as the total number of nodes N grows. Each simulation begins with a single infected individual, and the time is reset to zero after the number of infected individuals reaches ten, when counted across all compartments. This excludes simulations where the disease has died out before it becomes established in the population, and it also minimises the discrepancies between simulations and the approximations caused by random delays in the early epidemic phase. The results of these tests are presented in Fig. 1, which show the comparison of an average of 100 simulations (consisting of 20 simulations for five different random networks with the same topology) and the output from the pairwise model (1). Figure 1 shows that increasing the number of infectious stages leads to a more rapid spread of the disease with higher peak prevalence, despite the mean duration of infection remaining unchanged. This suggests that the lead time to implement any control measures is much shorter than estimates based on standard models where recovery is Poisson would suggest. This behaviour was also observed in the case of homogeneous populations [33]. We further note that for the same parameters of the disease dynamics, the trend of faster growth is even more profound for scale-free networks. This effect can be attributed to the influence of a small number of highly connected nodes; these individuals are at greater risk of receiving infection, and also have a much greater capacity to spread the disease, thereby causing a rapid increase in the number of new infections. This also has a significant impact on the threshold parameter which describes the point at which an epidemic occurs, as will be discussed later.

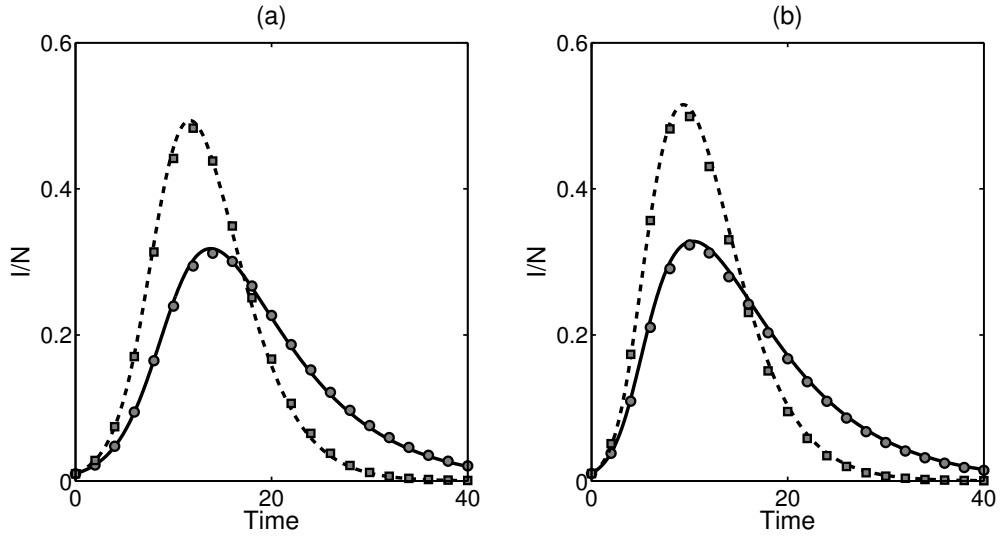

Figure 1: Dynamics of epidemics spreading on unclustered networks of 1000 nodes with (a) bimodal degree distribution with an even split of nodes having degrees 4 or 12, and (b) truncated scale-free degree distribution $P(k) \sim k^{-\alpha}$ bounded by $k_{min} = 4$, $k_{max} = 60$, and with $\alpha = 2.5$, and the mean degree of around 8. For both topologies, the simulations are performed for $K = 1$ (black line, circles) and $K = 4$ (dashed line, squares). Lines show the solution of the pairwise model (1) with the closures given in (8), and symbols correspond to stochastic network simulation. Other parameter values are $\tau = 0.07$, $\gamma = 0.15$.

2.2 Characteristics of the multi-stage compact model

2.2.1 Real-time epidemic growth rate

Now that the system of pairwise equations (1) with closures given in (8) has been shown to accurately match numerical simulations, we focus on deriving analytical results for this model. Some of the pertinent questions concerning the early behaviour of an outbreak are as follows: will a small initial number of infected individuals lead to a major outbreak amongst the population, and if so, how rapidly will the disease prevalence grow? Some insights into the early-stage disease dynamics can be obtained by performing a linear stability analysis of the disease-free equilibrium (DFE), where $[S] = N$, $[SS] = n_1 N$, $[I^{(j)}] = [SI^{(j)}] = [SR] = 0$, $j = 1, 2 \ldots, K$ of system (1) with the closure given in (8). The stability of the DFE and thus the early epidemic behaviour is determined by the eigenvalues, λ, of the Jacobian matrix $\mathcal{J} \in \mathbb{R}^{(2K+2)\times(2K+2)}$ ($[SR]$ can be safely excluded, as it only introduces a further row and column of zeros). Due to the nature of the system, $\mathcal{J}$ can be recast in the block form $\mathcal{J} = \begin{pmatrix} A & B \\ C & D \end{pmatrix}$, where A is a lower-diagonal $(K+2)\times(K+2)$ matrix, B is a $(K+2)\times K$ matrix, C is a zero $K \times (K+2)$ matrix, and D is a $K \times K$ matrix. This simplifies the calculations significantly, since the characteristic equation can now be rewritten as the product

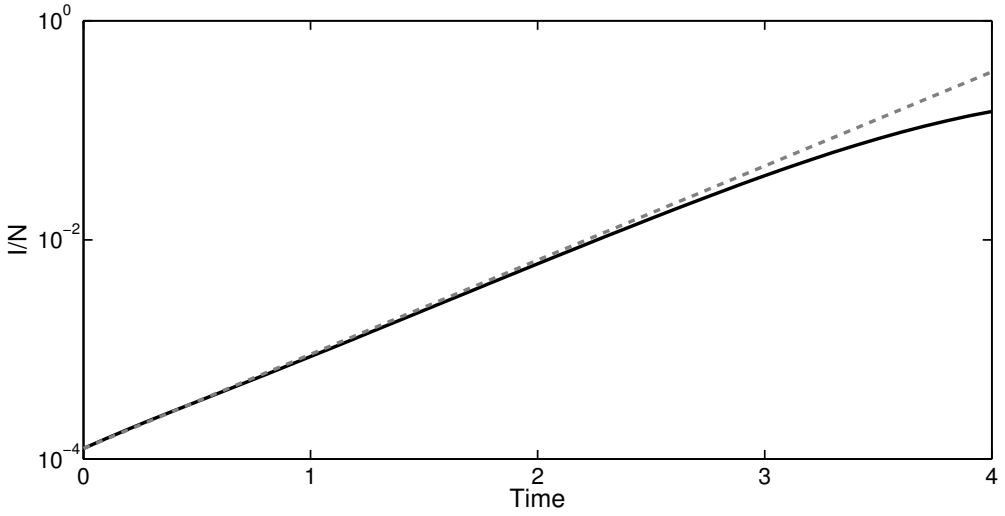

Figure 2: Dynamics of the early behaviour of a disease outbreak. The solid black line corresponds to the proportion of the infected population as described by system (1), and the dashed line shows the early solution approximated by the maximum eigenvalue of the DFE. Results are shown for an epidemic on a truncated scale-free network with $k_{min} = 4$, $k_{max} = 40$ and $\alpha = 2.81$. Disease parameters are $\tau = 0.3$, $\gamma = 1$, $K = 3$, with these and the chose network leading to $\lambda_{max} = 1.98$.

of diagonal elements of the matrix A multiplied by the determinant of the matrix D, i.e.

$$\lambda^2(\lambda + K\gamma)^K \begin{vmatrix} \tau n_1\zeta(0) - K\gamma - \tau - \lambda & \tau n_1\zeta(0) & & \dots & \tau n_1\zeta(0) \\ K\gamma & -K\gamma - \tau - \lambda & 0 & \dots & 0 \\ 0 & K\gamma & \ddots & \ddots & \vdots \\ \vdots & 0 & \ddots & \ddots & 0 \\ 0 & \dots & 0 & K\gamma & -K\gamma - \tau - \lambda \end{vmatrix} = 0. \qquad (10)$$

The maximum eigenvalue, λ_{max}, emerges from the determinant of D, as all other eigenvalues are either zero or negative. Once found in terms of system parameters, λ_{max} gives the initial exponential growth rate of the epidemic, and the number of infected individuals, close to $t = 0$, is well approximated by $[I](t) \approx [I](0)e^{\lambda_{max}t}$, where again $[I](t) = \sum_i [I]^{(i)}(t)$. To illustrate this, in Fig. 2 the early dynamics of an outbreak is shown against this early growth estimate. For sufficiently small time, the two solutions are almost indistinguishable, suggesting that λ_{max} does indeed provide an accurate characterisation of the early phase of disease spread.

2.2.2 Epidemic threshold

The next important question is under what conditions an epidemic can be avoided. Clearly, there will be no epidemic growth for $\lambda_{max} = 0$, thus the change in stability of the DFE can be used to determine a threshold for major outbreaks, which in this case can be done analytically through algebraic manipulations. Setting $\lambda = 0$ in the matrix (10) and reducing the matrix to a series of lower diagonal matrices gives a condition for this critical point

$$\begin{aligned}(\tau n_1\zeta(0) - K\gamma - \tau)(-K\gamma - \tau)^{K-1} + \\ \tau n_1\zeta(0)\left(\sum_{i=1}^{K-1}\left[(-1)^{K-i}(K\gamma)^{K-i}(-K\gamma - \tau - \lambda)^{i-1}\right]\right) = 0.\end{aligned} \qquad (11)$$

Rearranging this equation, one obtains a *threshold parameter* $\mathcal{R}$

$$\mathcal{R} := n_1 \frac{n_2 - n_1}{n_1^2} \widetilde{\tau} = \left(\frac{Var(P)}{\mathbb{E}(P)} + \mathbb{E}(P) - 1 \right) \widetilde{\tau}, \tag{12}$$

such that the stability of the DFE changes at $\mathcal{R} = 1$. In this expression P denotes the degree distribution, $\mathbb{E}(P)$ and $Var(P)$ are its mean and variance, respectively, and

$$\widetilde{\tau} := 1 - \left(\frac{K\gamma}{\tau + K\gamma} \right)^K. \tag{13}$$

This result is significant because $\mathcal{R}$ is a time-independent threshold parameter that has been derived by considering the real-time growth rate of the disease directly from the pairwise model. This parameter and the growth rate are strongly related, since $\lambda_{max} = 0$ if and only if $\mathcal{R} = 1$ (see, for example, [2] or [41]). The structure and purpose of $\mathcal{R}$ are similar to those of the basic reproductive ratio $\mathcal{R}_0$ in classical models, and indeed, it agrees perfectly with generation-based methods of deriving threshold conditions (see, for example [42]), as we briefly discuss below.

2.2.3 The generational approach

An alternative interpretation of $\widetilde{\tau}$ is that of the *transmissibility* of the disease, defined as the probability that infection will pass across a link from an infected to a susceptible node, when this pair is considered in isolation. Therefore, expression (13) can also be obtained by direct computation of this probability, which gives

$$\widetilde{\tau} := \int_0^\infty \left(1 - e^{-\tau x}\right) \frac{1}{(K-1)!} (K\gamma)^K x^{K-1} e^{-(K\gamma)x} dx = 1 - \left(\frac{K\gamma}{\tau + K\gamma} \right)^K.$$

This equivalent definition of $\widetilde{\tau}$ shows that the threshold condition for epidemic growth in our pairwise model is equivalent to generation-based approaches used to define $\mathcal{R}_0$. The factor in (12) describes the expected remaining degree of a newly infected node, and, thus, the potential number of secondary infections which it could generate in an otherwise wholly susceptible population.

Identifying this threshold through either method allows one to predict that for $\mathcal{R} < 1$ the epidemic will die out, and for $\mathcal{R} > 1$ the epidemic will develop in the deterministic model (1). This threshold translates to stochastic simulations, however, there is still a small possibility that an early disease die-out can occur even when $\mathcal{R} > 1$. Similarly, small epidemics may occur in some cases where $\mathcal{R} < 1$. It is important to note that although $\widetilde{\tau}$ emerges directly from the linear stability analysis, identifying it as the transmissibility restores the conventional interpretation of the threshold for epidemic spread as the expected number of secondary infections caused by a single infected individual in a fully susceptible population. In this way, our findings agree with the literature (see, for example, [43]).

An interesting result can be reached by considering $\mathcal{R}$ in the case of a scale-free distribution with $P(k) \sim k^{-\alpha}$ where $\alpha \leq 3$. In this case, unless $P(k)$ is truncated, higher moments n_2, n_3 of the degree distribution are not defined as the population size tends to infinity, and, hence, as the population size grows, the threshold parameter $\mathcal{R}$ will diverge for any non-trivial choice of the disease parameters τ, γ and K. Under these circumstances, the network topology dominates the dynamics of disease, and unless the contact structure can be altered or influenced, the disease will always spread through the population. This conclusion has been reached before in other models [14].

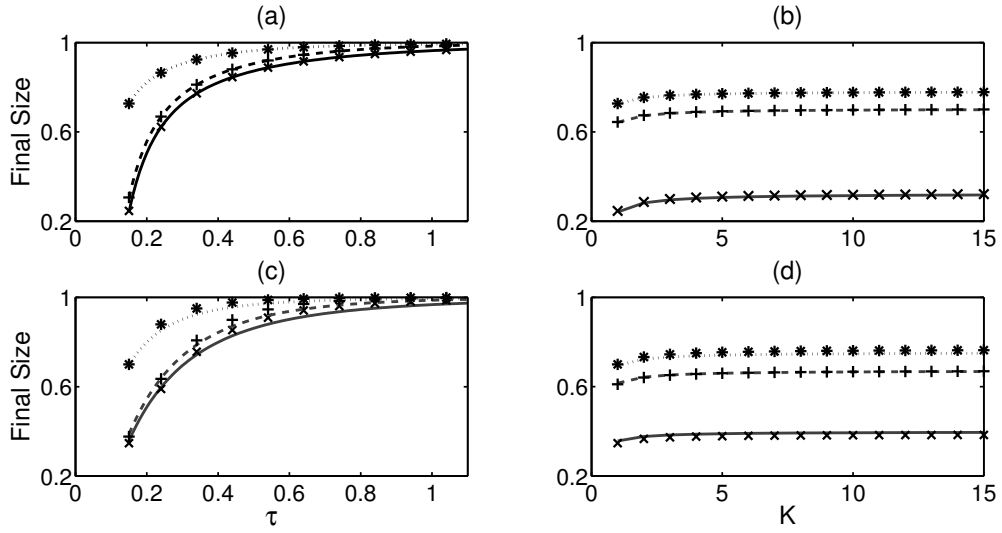

Figure 3: Comparison of the final epidemic size as determined by equations (14) and (15) (lines) and solutions of the pairwise model (1) (markers) for bimodal degree distribution an even split of nodes with degree 4 and 12 (a)-(b); and truncated scale-free networks with $\alpha = 2.5$ bounded between 4 and 60 (c)-(d), respectively. The parameter values are: (a), (c) $K = 1$, $\gamma = 1$ (solid line, crosses), $K = 4$, $\gamma = 1$ (dashed line, pluses), $K = 1$, $\gamma = 0.5$ (dotted line, stars); (b), (d) $\tau = 0.15$, $\gamma = 1$ (solid line, crosses), $\tau = 0.25$, $\gamma = 1$ (dashed line, pluses), $\tau = 0.15$, $\gamma = 0.5$ (dotted line, stars).

2.2.4 The final epidemic size

Since we are studying the spread of epidemics in a closed population, every epidemic will reach an end when there are no more infected individuals, at which point every member of the population is either still susceptible or in the removed class. To quantify the severity of an epidemic, it is instructive to look at the proportion of the population who will become infected over the entire lifetime of the epidemic; this quantity is known as the *final epidemic size*. In principle, it may be possible to manipulate the equations in (1) with the newly derived closure approximation (8) to find first-integral-like relations and thus find an expression for the final epidemic size [6, 33]. However, by considering the final epidemic size problem using a bond percolation model, [44] showed that it is possible to obtain an exact result for the mean final epidemic size. Based on the generating function for the degree distribution $G_0(x) := \sum_k p_k x^k$, where $P(k) = p_k$, the generating function for the excess degree distribution $G_1(x) = \frac{1}{n_1} G_0'(x) = \frac{1}{n_1} \sum_k k p_k x^{k-1}$, and the transmissibility, which for our model is given by $\widetilde{\tau}$ in (13), the final epidemic size is given by [44]:

$$\mathcal{R}_\infty = 1 - G_0(1 + (\theta - 1)\widetilde{\tau}) = 1 - \sum_k p_k (1 + (\theta - 1)\widetilde{\tau})^k, \tag{14}$$

where θ is the unique solution in $(0, 1)$ of the following equation

$$\theta = G_1(1 + (\theta - 1)\widetilde{\tau}) = \frac{1}{n_1} \sum_k p_k (1 + (\theta - 1)\widetilde{\tau})^{k-1}. \tag{15}$$

Newman's work has been revisited by [45], and whilst they showed that the distribution of final sizes suggested by Newman's original work was incorrect for non-constant infectious periods the mean final epidemic size given by (14) and (15) is correct.

Figure 3 shows the comparison of the final epidemic size results based on equations (14) and (15) to results from the numerical solution of the new pairwise model (1), and the agreement is excellent. It is noteworthy that in all cases the final epidemic size behaves as expected with respect to the disease parameters, i.e. a higher (lower) transmission rate τ results in a larger (smaller) final epidemic size, the mean duration of infection (γ^{-1}) has a similar effect, and a tighter distribution of the infectious periods (higher K) increases the predicted final epidemic size. Furthermore, a careful comparison of bimodal and truncated scale-free networks shows that having a broader degree distribution leads to certain differences in the dynamics. Namely, for relatively low transmission rates, epidemics of measurable size are predicted in truncated scale-free networks but not necessarily for the bimodal distribution. However, as the transmissibility grows (either through increasing τ or K) there comes a point where the final epidemic size becomes larger for the bimodal degree distribution. The most likely explanation for this is that poorly connected nodes are more difficult to reach in truncated scale-free networks, as once the highly connected nodes are infected the epidemic struggles to infect nodes with few links.

2.3 Limiting cases

It is instructive to look at the behaviour of model (1) in two particular limits of the number of infectious stages. When $K = 1$, model (1) reverts to the classical Markovian pairwise model which has been thoroughly studied [38, 46]. As the number of stages increases, the shape of the distribution for the infectious period changes, as shown in Fig. 4. For larger K one can see that the distribution grows tighter around the mean, which is kept constant at γ^{-1} due to the particular formulation of the model, and there is also much less variation in the duration of infection. The limiting case of $K \to \infty$ results in the infected period having a Dirac delta distribution $\delta\left(t - \gamma^{-1}\right)$ around the mean infectious period. It has been recently shown that this case can be accurately described by a system of pairwise delay differential equations (DDEs) for homogeneous populations [28], in which case the above-mentioned concept of transmissibility is also applicable. In this case, the transmission process is still Markovian (thus, the time to infection of a susceptible node with an infected neighbour is drawn from an exponential distribution with parameter τ), however, the infectious period is now constant, hence the probability of the infected node recovering is given by $\xi(t)$, where

$$\xi(t) = \begin{cases} 0 & \text{if} \quad 0 \leq t < \gamma^{-1}, \\ 1 & \text{if} \quad t \geq \gamma^{-1}. \end{cases}$$

Under these circumstances the transmissibility for a disease with a constant infectious period is given by

$$\widetilde{\tau}_{\text{const.}} = \int_0^\infty \tau e^{-\tau x} \xi(x) dx = 1 - e^{-\tau/\gamma}.$$

It is easy to show that taking the limit $K \to \infty$ in (13) yields the same result, i.e.

$$\lim_{K \to \infty} \widetilde{\tau} = 1 - e^{-\tau/\gamma}.$$

This suggests that results for the final epidemic size and the threshold parameter $\mathcal{R}$ for the case of a constant infectious period can be derived independently from the DDE system [28], and they coincide with the result of taking the limit as $K \to \infty$ for the multi-stage model (1). This model, therefore, bridges the gap between the traditional Markovian and delay-based scenarios, and accurately represents the spread of a disease with a distribution of infectious period which cannot be modelled by either.

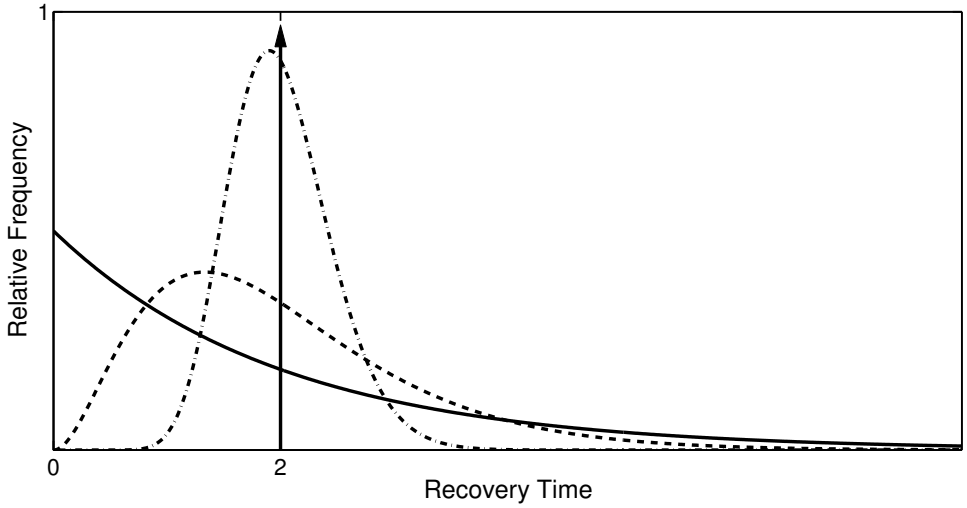

Figure 4: The distribution of infectious periods in the Markovian case of $K = 1$ (solid), for $K = 3$ (dashed), $K = 20$ (dash-dotted), and the Dirac delta distribution corresponding to $K = \infty$. The mean infectious period is equal to 2 for all four distributions.

3 The pairwise model on clustered networks

As has already been mentioned, clustering is known to play an important role in the spread of epidemics on networks. A convenient way to quantitatively characterise the level of clustering in a given network is through the clustering coefficient ϕ, most commonly defined as the proportion of closed triangles of nodes out of the total number of triples (open and closed together) in the network. The clustering coefficient ϕ can be intuitively understood as the probability of two nodes with a common neighbour being connected. This coefficient can be computed as follows [6]

$$\phi = \frac{\text{trace}(A^3)}{||A^2|| - \text{trace}(A^2)}, \tag{16}$$

where $A = (a_{ij})_{i,j=1,2,\ldots,N}$ is the adjacency matrix of the network, with $a_{ij} = a_{ji}$, $a_{ii} = 0$ for all i, j, $a_{ij} = 1$ if nodes i and j are connected and zero otherwise, and $||\cdot||$ stands for the sum of all the elements of the matrix. In the previous section it was assumed that $\phi = 0$. However, studies based on the data collected from real-world networks have found that this is often not the case. For example, studies of mathematics collaboration networks have found $\phi = 0.15$ [47], and similar studies for other disciplines have found that the clustering coefficient ranged from $\phi = 0.066$ to $\phi = 0.726$ [48], thus suggesting that clustering is often an important factor to be included in the network model.

The challenge presented by clustered networks is that one can no longer assume that all triples are open, and, therefore, the closures of pairwise models have to be reconsidered and appropriately modified to effectively approximate the dynamics. In the most general formulation, one can start from a triple $[X_a S_b Y_c]$ where the degree of nodes is considered explicitly. Based on [46], we can write

$$[X_a S_b Y_c] \approx \frac{b-1}{b} \frac{[X_a S_b][S_b Y_c]}{[S_b]} \left(1 - \phi + \phi \frac{n_1 N}{ac} \frac{[X_a Y_c]}{[X_a][Y_c]}\right), \tag{17}$$

where again $X, Y \in \mathbb{S}$. In order to remove the dependency on node degree, we employ two *a priori* approximations first introduced by [38]. The first of these approximations has already featured

earlier in (4), namely,

$$[X_aY] \approx \frac{a[X_a]}{\sum_j j[X_j]}[XY],$$

and the second has the form

$$[X_aY_b] \approx \frac{[X_aY][XY_b]}{[XY]}\frac{[ab]n_1N}{a[a]b[b]} \approx \frac{[X_aY][XY_b]}{[XY]}, \tag{18}$$

where n_1 is the mean degree, and $[a]$ is the expected number of individuals with degree a in the network. The new approximation assumes that the joint probability of a pair can be accurately estimated by removing dependence on the degree of the second node and multiplying by a second term that captures the specifics of the network structure. This term is known as the *assortativity* of nodes with degrees a and b, and it measures whether nodes with similar degrees are more likely or less likely to connect to each other [49]. The simplification shown in (18) assumes null assortativity (i.e. random connection between nodes) and will be used throughout this section.

We are now in a position to derive closures for the multi-stage model on clustered networks. In (17) the terms outside the bracket are similar to the closure in (8) and (9) for unclustered networks. In fact, the sum over all degrees a and c will result in the same expression but with the subscripts dropped, as can be checked using (4) and (18). Thus, the first part of the derivation follows exactly the same methodology as for the unclustered network case discussed in Section 2. Focusing on the final term in (17), which is responsible for clustering, we use the above approximations to obtain

$$\begin{aligned}\frac{n_1N}{ac}\frac{[X_aY_c]}{[X_a][Y_c]} &\approx \frac{n_1N}{ac}\frac{[X_aY]}{[XY][X_a]}\frac{[XY_c]}{[Y_c]} \approx \frac{n_1N}{ac}\frac{a[X_a][XY]}{[XY][X_a]\sum_i i[X_i]}\frac{[XY_c]}{[Y_c]},\\ &\approx \frac{n_1N}{c}\frac{1}{\sum_i i[X_i]}\frac{c[Y_c][XY]}{[Y_c]\sum_j j[Y_j]} \approx n_1N\frac{[XY]}{\sum_i i[X_i]\sum_j j[Y_j]}.\end{aligned}$$

In a similar way as it was done for T_1, it is possible to define $J_1^{(i)}$ and P_1 as the sums of all edges emanating from infected nodes in the i-th stage and from removed nodes, respectively. Then $J_1 = \sum_{j=1}^{K} J_1^{(j)}$ is the number of edges emanating from *all* infected nodes, regardless of their degree and the stage of the disease which they are in. The full closures necessary for the model with clustering can now be stated as follows,

$$\begin{aligned}[SSI] &= \zeta(t)\frac{[SS][SI]}{[S]}\left(1-\phi+\phi n_1N\frac{[SI]}{T_1J_1}\right),\\ [ISI^{(i)}] &= \zeta(t)\frac{[IS][SI^{(i)}]}{[S]}\left(1-\phi+\phi n_1N\frac{[II^{(i)}]}{J_1J_1^{(i)}}\right), \quad \text{for} \quad i=1,2,\ldots,K,\\ [ISR] &= \zeta(t)\frac{[SI][SR]}{[S]}\left(1-\phi+\phi n_1N\frac{[IR]}{J_1P_1}\right),\end{aligned} \tag{19}$$

where $\zeta(t)$ is still given by (9), and we have defined

$$T_1 = [SS] + \sum_{i=1}^{K} [SI^{(i)}] + [SR],$$
$$J_1^{(j)} = [SI^{(j)}] + \sum_{i=1}^{K} [I^{(i)} I^{(j)}] + [I^{(j)} R], \qquad J_1 = \sum_{j=1}^{K} J_1^{(j)},$$
$$P_1 = [SR] + \sum_{i=1}^{K} [I^{(i)} R] + [RR].$$

The model now has to explicitly consider every possible combination of pairs, which, for a disease with a K-stage gamma distributed infectious period, yields the following system of $(K^2 + 3K + 4)$ equations

$$\begin{aligned}
&[\dot{S}] = -\tau[SI], \\
&[\dot{I^{(1)}}] = \tau[SI] - K\gamma[I^{(1)}], \\
&[\dot{I^{(j)}}] = K\gamma[I^{(j-1)}] - K\gamma[I^{(j)}], \quad \text{for} \quad j = 2, 3, \ldots, K, \\
&[\dot{SS}] = -2\tau[SSI], \\
&[\dot{SI^{(1)}}] = -(\tau + K\gamma)[SI^{(1)}] + \tau\left([SSI] - [ISI^{(1)}]\right), \\
&[\dot{SI^{(j)}}] = -(\tau + K\gamma)[SI^{(j)}] + K\gamma[SI^{(j-1)}] - \tau[ISI^{(j)}], \quad \text{for} \quad j = 2, 3, \ldots, K, \\
&[\dot{SR}] = -\tau[ISR] + K\gamma[SI^{K}], \\
&[\dot{I^{(1)}I^{(1)}}] = 2\tau[SI^{(1)}] + 2\tau[ISI^{(1)}] - 2K\gamma[I^{(1)}I^{(1)}], \\
&[\dot{I^{(1)}I^{(j)}}] = \tau[SI^{(j)}] + \tau[ISI^{(j)}] + K\gamma\left([I^{(1)}I^{(j-1)}] - 2[I^{(1)}I^{(j)}]\right), \quad \text{for} \quad j = 2, 3, \ldots, K, \\
&[\dot{I^{(j)}I^{(k)}}] = K\gamma\left([I^{(j-1)}I^{(k)}] + [I^{(j)}I^{(k-1)}] - 2[I^{(j)}I^{(k)}]\right), \quad \text{for} \quad j, k = 2, 3, \ldots, K, \\
&[\dot{I^{(1)}R}] = \tau[ISR] + K\gamma\left([I^{(1)}I^{(K)}] - [I^{(1)}R]\right), \\
&[\dot{I^{(j)}R}] = K\gamma\left([I^{(j)}I^{(K)}] + [I^{(j-1)}R] - [I^{(j)}R]\right), \quad \text{for} \quad j = 2, 3, \ldots, K, \\
&[\dot{RR}] = 2K\gamma[I^{(K)}R],
\end{aligned} \tag{20}$$

with the closures for $[SSI]$, $[ISI^{(j)}]$ and $[ISR]$ given in (19). Note that, as one would expect, setting $\phi = 0$ reduces this model back to the simpler compact model introduced and discussed in Section 2.

3.1 Numerical Simulations

To investigate the accuracy of model (20), we compare its output to stochastic network simulation. First, it is necessary to explain how one can construct clustered networks, which is achieved using the *big-V rewiring* method [50]. This algorithm takes as an input a random unclustered network constructed with the configuration model, and at each iteration it looks for a chain of five nodes $u - v - x - y - z$, such that newly created links after the rewiring process do not yet exist. Once such a chain is found, the algorithm deletes $u - v$ and $y - z$ edges, and connects $v - y$ and $u - z$ in order to replace the five-node chain with a triangle and a separately connected edge. If this

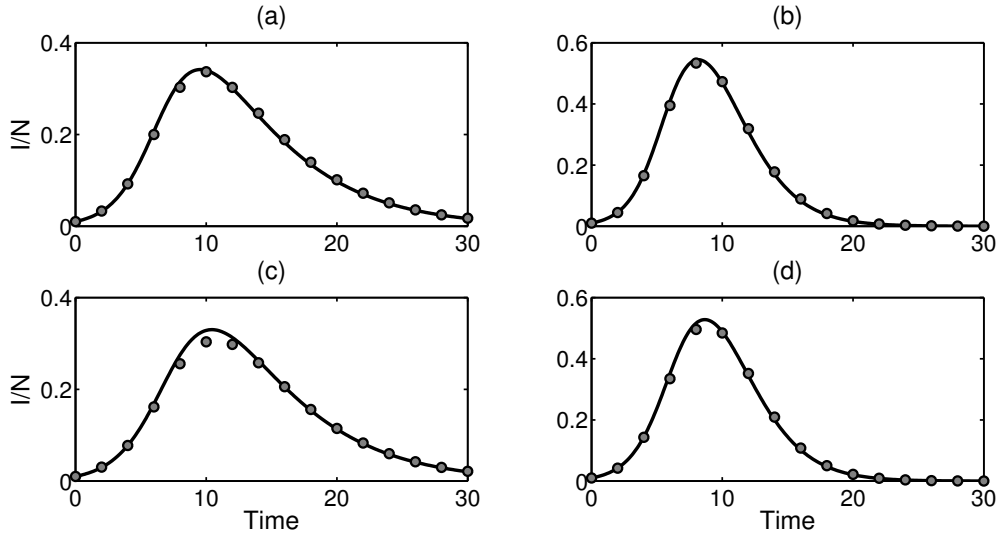

Figure 5: Comparisons of numerical results (circles) and the compact pairwise (solid line) model on a network with an even split of nodes having degrees 4 and 12. (a) $K = 1$, $\phi = 0$; (b) $K = 5$, $\phi = 0$; (c) $K = 1$, $\phi = 0.2$; (d) $K = 5$, $\phi = 0.2$. Other parameter values are τ=0.1, $\gamma = 0.2$.

procedure increases local clustering, then the rewiring is accepted, and the algorithm continues until the target clustering coefficient ϕ is reached. The benefit of this approach is that while the level of clustering can be varied, the degree distribution remains the same.

Many other algorithms exist that can be used to generate clustered networks, with some of these algorithms using subgraphs to construct the overall network [51, 52, 22, 23, 21, 20, 24, 53]. The subgraphs over three, four or more nodes typically display different levels of clustering, and thus, global level of clustering can be tuned. The probability generating function formalism leads to percolation models [51, 21] or ODE [23, 24] that agree well with explicit stochastic network simulation on particular clustered networks. Further methods exist to generate clustered networks [54, 55, 56], however, the big-V algorithm introduces triangles in a random and uniform way, generating little structure beyond triangles at low and medium levels of clustering. Of course, for high levels of clustering most algorithms lead to fragmentation of the network into disconnected components, and, as a result, densely connected subgraphs may emerge. Using a subgraph counting procedure, [20, 24, 53] have shown that networks generated using the big-V algorithm have a negligibly small number of subgraphs over four or more nodes when compared to networks generated based on subgraphs. Given that pairwise models operate on the basis of closures at the level of open triples and triangles, and that they make no further assumptions about higher-order structure, clustered networks generated using the big-V algorithm are ideal for comparison between explicit stochastic network simulation and pairwise models.

Figure 5 illustrates the results of simulations on networks with a bimodal degree distribution both for unclustered networks, and for rewired networks with the clustering coefficient $\phi = 0.2$, which is in the range observed in empirical data [48, 47]. Whilst the agreement is good in all cases, the clustering introduces some inaccuracy. This is to be expected since the number of susceptible neighbours of a node is now harder to predict due to the presence of short cycles. Furthermore, the inclusion of triangles appears to slow down the spread of the epidemic. The grouping of nodes into small communities decreases the number of individuals at risk of infection at any time, because the disease has fewer routes to spread away from an infectious seed. One should also note

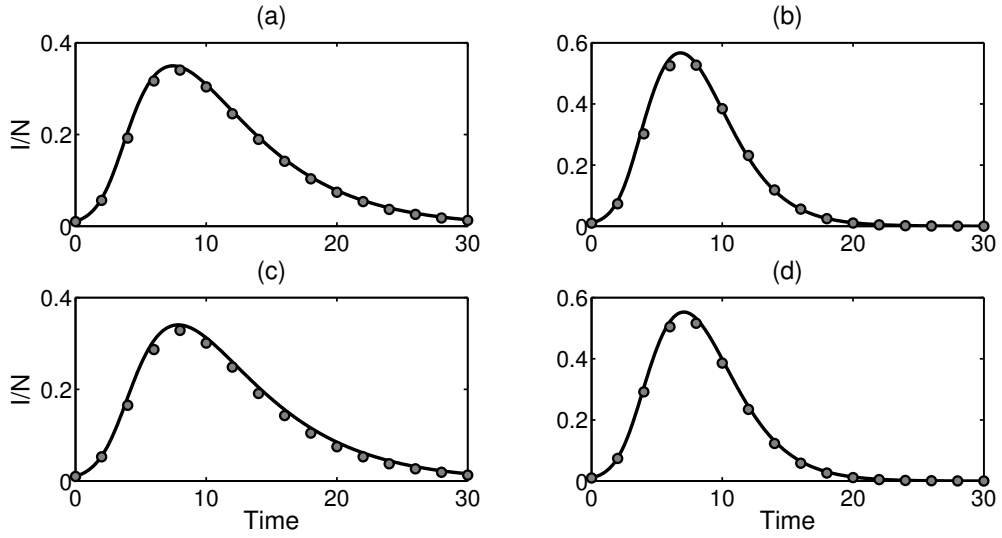

Figure 6: Comparisons of numerical simulations (circles) to the pairwise model (solid line) for truncated scale-free networks with exponent $\alpha = 2.5$, $k_min = 4$, $k_max = 60$. (a) $K = 1$, $\phi = 0$; (b) $K = 5$, $\phi = 0$; (c) $K = 1$, $\phi = 0.2$; (d) $K = 5$, $\phi = 0.2$. Other parameter values are τ=0.1, $\gamma = 0.2$.

that with the introduction of a gamma-distributed infectious period, the trend of faster epidemic growth and higher peak prevalence with increasing values of K is preserved. This reinforces the earlier conclusion that the inclusion of a more realistic distribution of infectious periods can lead to more rapid severe epidemics than what would be predicted by the traditional models with an exponentially distributed infectious period.

Similar changes in the dynamics are observed in the case of truncated scale-free networks, as shown in Fig. 6. However, unlike the bimodal case, the impact of higher clustering has a less pronounced effect on the timescale of the epidemic. This is likely due to the fact that highly connected nodes cannot be effectively restricted to a single small community, and, therefore, their ability to spread the disease is not significantly affected. It can also be seen that a larger value of K appears to improve the accuracy of the pairwise model (20).

Despite its successes, the pairwise model (20) becomes less accurate as clustering in the network increases. To investigate this in more detail, we have performed numerous comparisons between simulations and the numerical solution to the pairwise model (20) for networks with bimodal and truncated scale-free degree distributions, with increasing levels of clustering. The results of these tests are presented in Fig. 7 which shows that system (20) is reasonably accurate for low levels of ϕ, however, this accuracy reduces as ϕ increases. The most likely explanation for this reduction in model accuracy is the assumption of null assortativity explicitly made in (18) when deriving closures for the clustered model, since it is known that clustering in networks increases assortativity [17]. Furthermore, it has also been shown in a number of earlier studies that high levels of assortativity are the norm in real social networks (see, for example, [57]). Since the null assortativity assumption is violated in such networks, it is not surprising that the pairwise model (20) does not provide an accurate representation of dynamics for high levels of clustering.

Figure 8 shows the comparison of the final epidemic size recorded from the simulations and the pairwise model. Again, it is clear that the pairwise model performs worse for high levels of clustering. However, the results suggest that when clustering is present in the network, the epidemic threshold appears to increase, and thus measurable epidemics are less likely to occur.

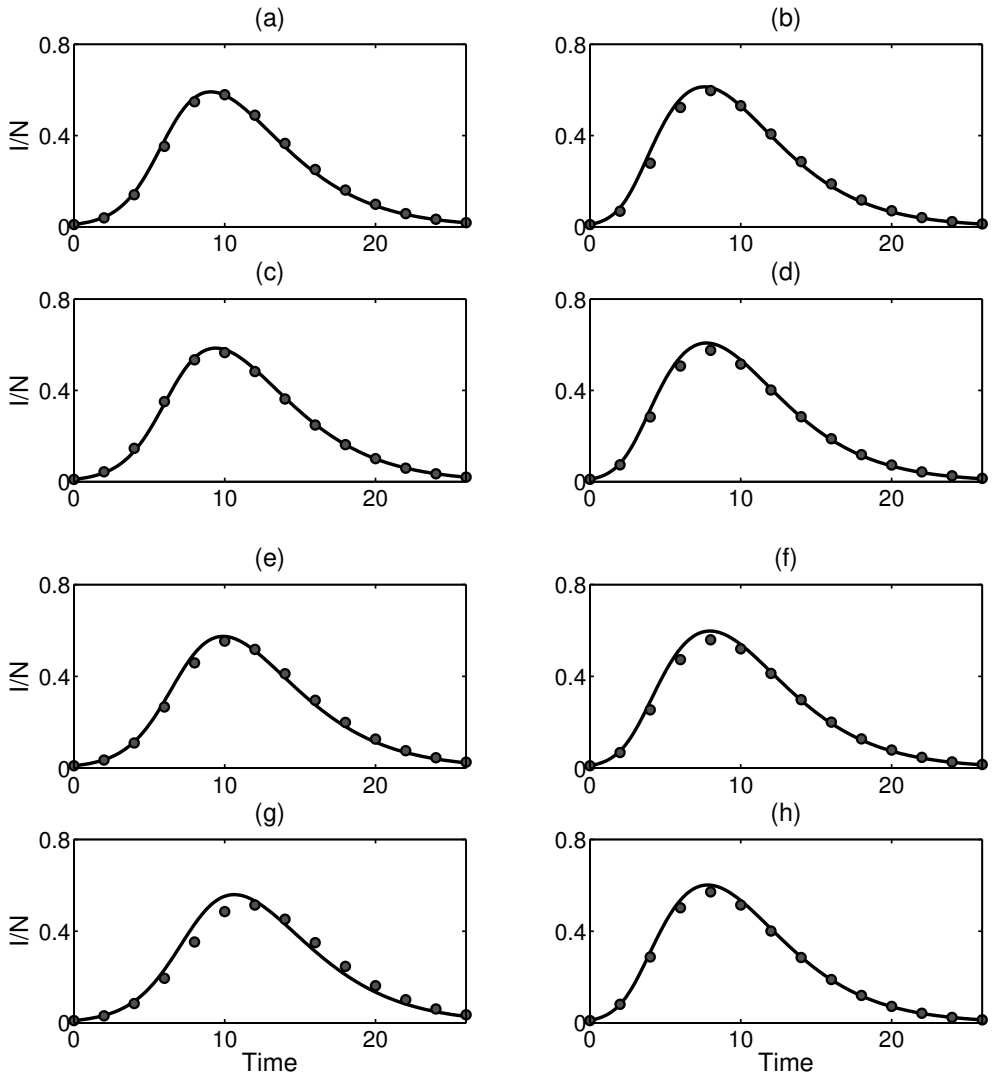

Figure 7: Comparison between the clustered pairwise model (20) (solid lines) and network simulation (circles) for different values of the clustering coefficient ϕ. The left column shows results for networks with bimodal degree distribution having an even split of nodes with degrees 4 or 12, the right column shows the results for truncated scale-free networks with the exponent $\alpha = 2.5$ and node degrees bounded between $k_{min} = 4$ and $k_{max} = 60$. Parameter values are $\tau = 0.1$, $\gamma = 0.15$, $K = 3$, with ϕ increasing through 0.1, 0.2, 0.3, 0.4 from top to bottom. As the clustering ϕ increases beyond 0.2, the inaccuracy of the clustered pairwise model becomes more pronounced.

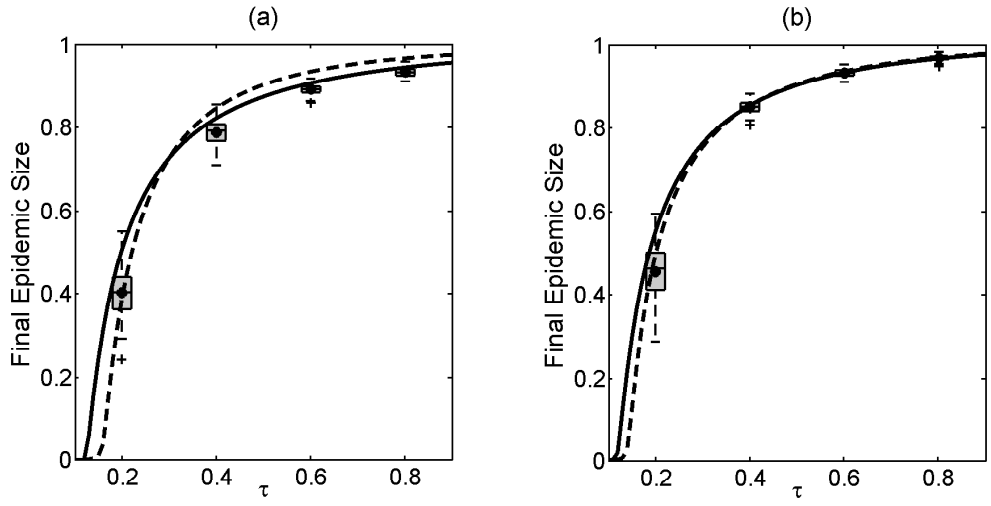

Figure 8: Dependence of the final epidemic size on the per-link transmission rate for networks with bimodal degree distribution of degree 4 or 12, split equally. The parameter γ is fixed at 1, and in (a) $K = 1$, (b) $K = 4$. Solid lines correspond to epidemics on unclustered networks, dashed lines illustrate equivalent epidemics on a network with $\phi = 0.4$, all based on pairwise models. The boxplots illustrate the results from 100 numerical simulations for each highlighted value of τ. The box shows the lower and upper quartile, and horizontal line within the box shows the median. The whiskers extend to a maximum distance of 1.5 times the interquartile range, and crosses represent outliers. Black circles denote the mean final epidemic size.

This can be seen in Fig. 8, as a higher transmission rate is required in order for the final epidemic size to diverge away from zero when the epidemic takes place in a clustered network. Similarly, for clustered networks, simulation results show that the final epidemic size will be reduced when compared to equivalent networks with the same degree distribution, no clustering and the same parameters of the disease dynamics. This makes sense intuitively, since rewiring a network makes the population more segregated and thus there exist clusters of individuals that are more likely to escape infection. It is noteworthy that the data in Fig. 8 (b) is grouped much more tightly, showing that the reduced variance in the distribution of recovery times is reflected in the reduced variance of the distribution of final epidemic sizes from simulation data. This is illustrated by the significantly smaller spread of the box-and-whisker plots for the non-Markovian case. Lower variance in the final epidemic size occurs alongside improved agreement between pairwise and simulation model, both for unclustered (1) and clustered models (20). This suggests that pairwise approximations perform better for diseases with smaller variance of the distribution of recovery times, and that clustering may play a less significant role when non-Markovian distributions are introduced.

In an extensive recent study of small/toy networks, [58] proved that for an SIR epidemic on a single open triple or closed triangle the classical closures, such as those given in (3) and (17), are exact for constant infectious periods (see Proposition 3 in [58]). As has been previously discussed in Section 2.3, as the number of stages, K, increases in the pairwise model, we approach the limit of a constant infectious period. Although the exact results do not carry over to large networks, they suggest that a greater accuracy may be achieved on larger networks when the infectious period tends towards a fixed length, that is, as K increases. To test the validity of this hypothesis, in Fig. 9 we plot the value of the error between the final epidemic size computed from the pairwise model (20)

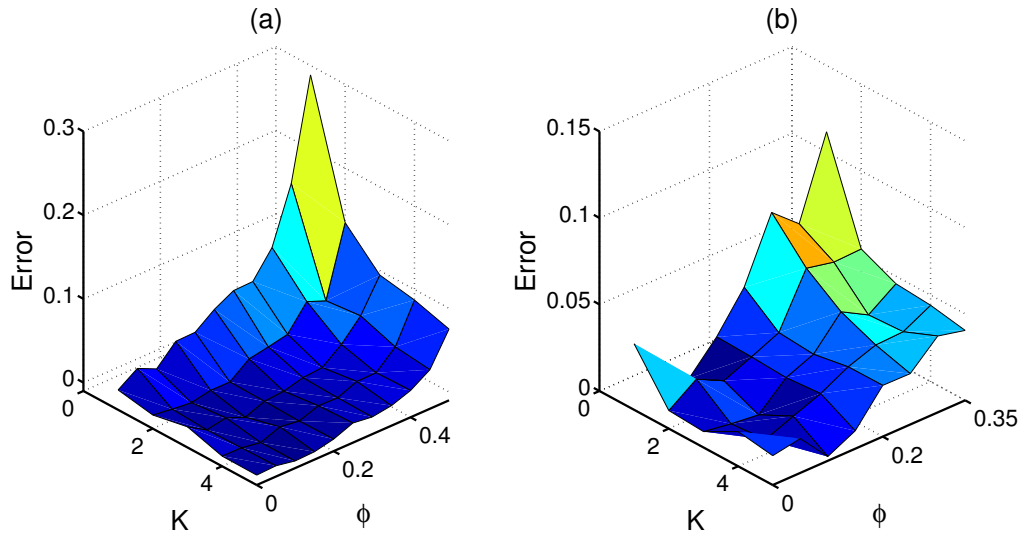

Figure 9: The error between the final epidemic sizes obtained from the solution of the pairwise model (20) and from the average of 100 numerical simulations plotted against the clustering coefficient ϕ and the number of stages of infection K, plotted as result from the pairwise model less result from simulation. Parameter values are $\tau = 0.3$, $\gamma = 1$. (a) A network with bimodal degree distribution, an even split of nodes having degrees $k_1 = 4$ and $k_2 = 12$. (b) A scale-free network of 1000 nodes with $k_{min} = 4$, $k_{max} = 60$, and $P(k) \sim k^{-2.5}$. Note that as predicted, even in the presence of clustering, as K grows, the error becomes smaller, and hence the pairwise model becomes more accurate.

and the results of 100 simulations under the same parameters, for the two model networks. Figure 9 indicates that the error does indeed decrease for any ϕ as the infectious period becomes tighter around the mean (as characterised by an increasing K), thus suggesting that the findings of [58] are also relevant for larger networks where both open and closed triples are present. Furthermore, one should note that in all but two cases the pairwise model (20) over-estimates the final epidemic size when compared to simulations. This suggests that in most cases the model can be expected to give an upper bound on the size of an epidemic. Even though our newly derived compact closures (19) are not exact, their performance improves greatly when the infectious period approaches the limit of a fixed infectious period. This is an important result that justifies the continued use of pairwise-like methods for non-Markovian epidemics on networks.

4 Discussion

In this paper we have derived and studied a new pairwise model for the spread of infectious diseases which includes three major characteristics that are not consistently studied concurrently, despite being essential for understanding disease dynamics in many realistic scenarios. Our pairwise model can account for degree heterogeneity, clustering and gamma-distributed infectious periods, and the number of equations in the pairwise model does not depend on the range of different node degrees. This approach follows the methodology of the so-called *compact pairwise models* [34, 36], and the output from the resulting pairwise model shows excellent agreement with results of numerical simulation for networks with either no or low levels of clustering, and for all the different degree distributions that have been considered.

The major heuristic assumption behind the super compact moment closure approximation is the existence of a linear relationship between the degree distribution of the starting network and the degree distribution of susceptible nodes as the epidemic evolves. According to [34], this linear relationship amounts to having $s_k(t)/P(k) = A(t)k + B(t) = q_k(t)$, for all $t \geq 0$, which essentially means that the degree distribution of the susceptible nodes can be deduced from $P(k)$ by using a multiplicative factor that is linear in k and whose gradient and intercept depend on time. In order to test this assumption explicitly, in Figs. 10 and 11 we check if the points $(k, s_k/P(k))$, for $k = k_{min}, k_{min+1}, \ldots, k_{max} - 1, k_{max}$, do indeed lie on a line at various points of the unfolding epidemic. The two figures illustrate that the linear relationship appears to be fulfilled to the same degree for both the standard Markovian model ($K = 1$) and the non-Markovian multi-stage model (here $K = 3$). To be more precise, it is obvious that $s_k/P(k)$ shows a strong linear relation for early time (shown in panels (b) and (c) of Fig. 10 and panel (b) of Fig. 11); although for latter stages of the epidemic the relation weakens as the number of susceptible nodes of high degree is depleted to a larger extent compared to susceptible nodes of lower degree. However, it is noteworthy that this deviation from the assumption does not significantly affect the accuracy of the pairwise model when compared to explicit stochastic network simulations, see panel (a) in Figs. 10 and 11.

For networks with bimodal degree distribution, as studied in the paper, we have that the distribution of the susceptible nodes satisfies the equations below

$$s_{k_1} + s_{k_2} = 1, \tag{21}$$

$$k_1 s_{k_1} + k_2 s_{k_2} = n_S, \tag{22}$$

where the system provides a unique solution for (s_{k_1}, s_{k_2}) without the need to use the linear approximation assumption, see also [34]. Hence, for this case, replicating the test in Figs. 10 and 11 is not warranted as it would neither confirm nor reject the validity of the assumption.

Overall, it would be desirable to carry out further tests to understand how (a) network properties and (b) the type of dynamics impact on the linearity assumption. For example, if the network is assortative, in which case nodes of the same or similar degree are more likely to be connected, will the same relation hold? The same could be considered in the context of disassortative networks, where nodes of differing degrees are more likely to be connected. The accuracy of the pairwise model when compared to simulation provides strong support for using the super compact closure at least for the class or family of networks presented in the paper. However, the fact that the departures from the linearity assumption seem not to impact significantly on the agreement between the mean-field and simulation models remains a question that warrants further investigation.

In the absence of clustering we have used linear stability analysis to determine a threshold parameter from the pairwise model, and we have shown that existing methods for finding the final epidemic size [44] can be applied. Equivalent results have not been found in the case of clustered networks. However, extensive numerical simulations have shown that introducing multiple stages of infection increases the speed of epidemic spread, as well as the peak prevalence and the final epidemic size. The interactions of degree heterogeneity, clustering and the distribution of infectious period all have significant yet contrasting impacts on an outbreak. For example, we have seen that both degree heterogeneity and a larger number of infectious stages (corresponding to a tighter distribution for the duration of infection) increase the growth rate of the epidemic in the early stages, however, this is countered when one includes clustering that is likely to be present in real contact networks. These findings are consistent with earlier results on the effects of clustering on the spread of epidemics [59]. [60] have shown that whilst clustering makes epidemics less likely, for scale-free topologies, and in the limit of infinite networks, an epidemic threshold does not exist, and a significant outbreak will always occur. The complexity of the pairwise model for clustered

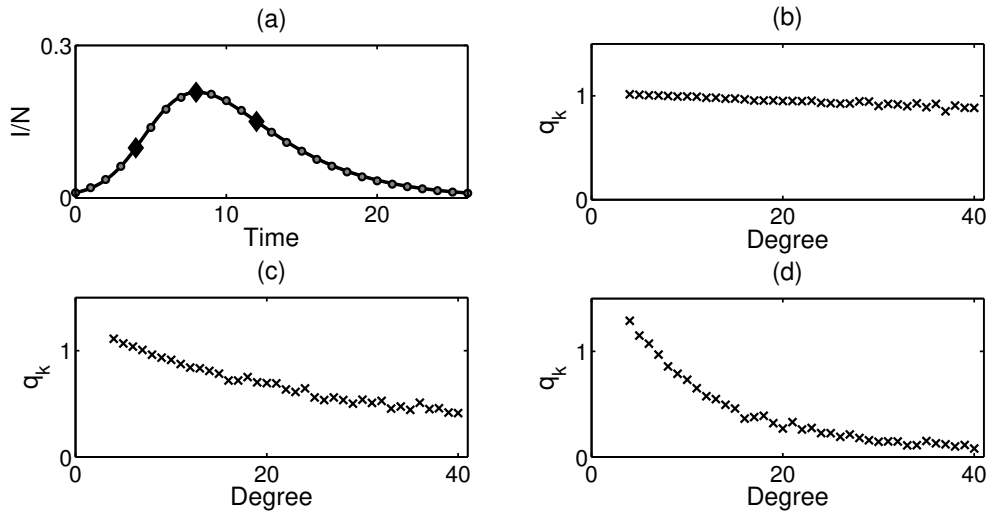

Figure 10: The results of exploring the $s_k(t)/P(k) = A(t)k+B(t)$ relation for a given epidemic. The curves shown in (a) are the solutions of the pairwise model (1) (solid line) and simulation results (grey circles) for an epidemic on a truncated scale-free network with $\alpha = 2.5$, with the degrees bounded between 4 and 40, and disease parameter values $\tau = 0.1$, $\gamma = 0.3$, $K = 1$. Diamonds at time $t = 4, 8, 12$ correspond to the points in time where the relationship is tested, the results of which are shown in (b), (c) and (d), respectively.

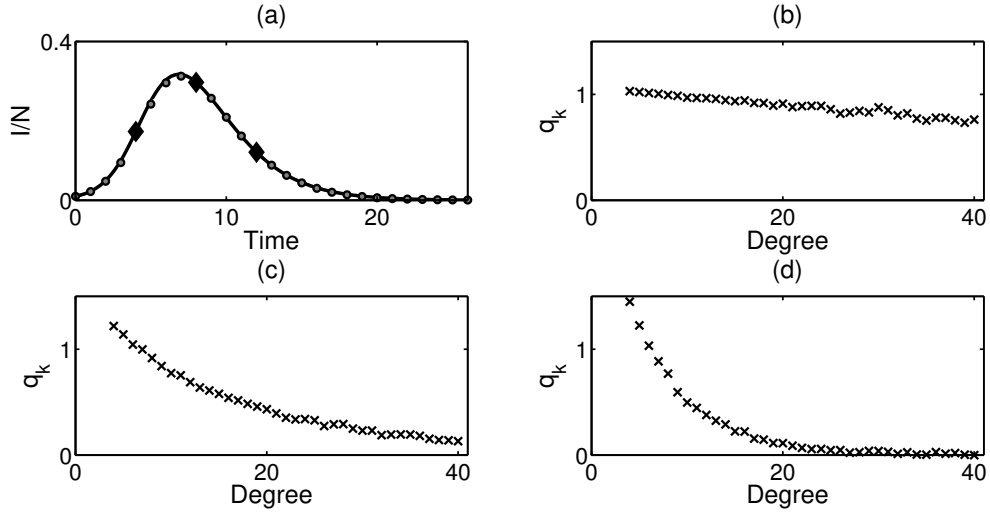

Figure 11: The results of exploring the $s_k(t)/P(k) = A(t)k + B(t)$ relation for a given epidemic. The curves shown in (a) are the solution of the pairwise model (1) and simulation results (grey circles) for an epidemic on a truncated scale-free network with $\alpha = 2.5$, with the degrees bounded between 4 and 40; with disease parameters $\tau = 0.1$, $\gamma = 0.3$, $K = 3$. Diamonds at time $t = 4, 8, 12$ correspond to the points in time where the relationship is tested, the results of which are shown in (b), (c) and (d), respectively.

networks has meant that analytical expressions for the epidemic threshold and the final epidemic size have not been found. In fact, analytical results have so far only been obtained for clustered networks with a specific construction, e.g. non-overlapping triangles [21]. Random rewiring enforces fewer restrictions on the network and thus allows for more complex topologies to emerge, which is likely to provide more realistic but also more challenging scenarios for modelling than networks with a prescribed nature of clusters.

A strength of the final pairwise model which we have presented is that it can be tuned based on the characteristics of the disease and population being studied. There are several ways to include more features into this model. For example, by allowing the transmission rate to vary depending on the stage of infection, one could model diseases with varying infectivity. Setting $\tau = 0$ in any number of initial stages also opens the possibility for multi-stage $SEIR$ models to be studied, again without altering the basic framework of the model.

Models, such as the one presented in this paper, could also be used for a more thorough study of the performance of closures and for mapping out how different approximations behave under different regimes, such as stochastic models for the transmission and recovery processes. Furthermore, one could consider whether non-Markovian transmission processes can be incorporated into pairwise or pairwise-like models. Additional motivation for research into this area comes from studies which have suggested that human contact patterns are typically very 'bursty' [61, 62]. This means that there are many short periods with high levels of interaction and longer periods of little or no action, and this may have a significant impact on how an epidemic may spread. It is possible that attempts to incorporate non-Markovian transmission may lead to a more complex system of integro-differential equations.

There have been many recent developments in the area of dynamic or adaptive networks [63, 64, 65, 66] where pairwise models have been used successfully to couple the dynamics of an epidemic on the network with the dynamics of the network. These models have shown that using pairwise approximation techniques it is possible to capture non-trivial properties of both network and epidemic dynamics in a single model. There is a wide scope for further research focussed on modelling the rewiring process, as well as for analysis of a reaction of networks to a spreading epidemic when considered as a non-Markovian process.

The pairwise model presented in this paper does well at accounting for non-Markovian infectious periods, indeed, it becomes more accurate in this case, yet it is limited in capturing epidemics on realistic clustered networks. This work highlights some of the important factors in modelling disease outbreaks, each of which can significantly alter the behaviour of an epidemic, and shows that model realism and complexity are correlated.

Acknowledgements

Neil Sherborne acknowledges funding for his PhD studies from EPSRC (Engineering and Physical Sciences Research Council), EP/M506667/1, and the University of Sussex. The authors would also like to thank the anonymous referees for their helpful comments and suggestions.

References

[1] R. M. Anderson and R. M. May, *Infectious Diseases of Humans*, vol. 1. Oxford University Press, Oxford, 1991.

[2] O. Diekmann, H. Heesterbeek, and T. Britton, *Mathematical Tools for Understanding Infectious Disease Dynamics*. Princeton University Press, Princeton, 2012.

[3] R. Pastor-Satorras, C. Castellano, P. Van Mieghem, and A. Vespignani, "Epidemic processes in complex networks," *Rev. Mod. Phys.*, vol. 87, pp. 925–979, 2015.

[4] N. M. Ferguson, D. A. T. Cummings, C. Fraser, J. C. Cajka, P. C. Cooley, and D. S. Burke, "Strategies for mitigating an influenza pandemic," *Nature*, vol. 442, no. 7101, pp. 448–452, 2006.

[5] G. Chowell and H. Nishiura, "Transmission dynamics and control of Ebola virus disease (EVD): a review," *BMC Medicine*, vol. 12, no. 1, p. 196, 2014.

[6] M. J. Keeling, "The effects of local spatial structure on epidemiological invasions," *Proc. R. Soc. B.*, vol. 266, no. 1421, pp. 859–867, 1999.

[7] L. Danon, A. P. Ford, T. House, C. P. Jewell, M. J. Keeling, G. O. Roberts, J. V. Ross, and M. C. Vernon, "Networks and the epidemiology of infectious disease," *Interdisciplinary perspectives on infectious diseases*, vol. (2011), 2011.

[8] M. J. Keeling and K. T. Eames, "Networks and epidemic models," *J. R. Soc. Interface*, vol. 2, no. 4, pp. 295–307, 2005.

[9] F. Liljeros, C. R. Edling, L. A. N. Amaral, H. E. Stanley, and Y. Åberg, "The web of human sexual contacts," *Nature*, vol. 411, no. 6840, pp. 907–908, 2001.

[10] W. Kermack and A. McKendrick, "A contribution to the mathematical theory of epidemics," *Proc. R. Soc. A*, vol. 115, pp. 700–721, 1927.

[11] P. Erdős and A. Rényi, "On random graphs I," *Publ. Math. Debrecen*, vol. 6, pp. 290–297, 1959.

[12] D. Brockmann, L. Hufnagel, and T. Geisel, "The scaling laws of human travel," *Nature*, vol. 439, no. 7075, pp. 462–465, 2006.

[13] G. Caldarelli, R. Marchetti, and L. Pietronero, "The fractal properties of Internet," *Europhys. Lett.*, vol. 52, no. 4, pp. 386–391, 2000.

[14] R. Pastor-Satorras and A. Vespignani, "Epidemic spreading in scale-free networks," *Phys. Rev. Lett.*, vol. 86, no. 14, pp. 3200–3203, 2001.

[15] A. James, J. W. Pitchford, and M. J. Plank, "An event-based model of superspreading in epidemics," *Proc. R. Soc. B*, vol. 274, no. 1610, pp. 741–747, 2007.

[16] M. E. J. Newman, S. H. Strogatz, and D. J. Watts, "Random graphs with arbitrary degree distributions and their applications," *Phys. Rev. E*, vol. 64, no. 2, p. 026118, 2001.

[17] D. V. Foster, J. G. Foster, P. Grassberger, and M. Paczuski, "Clustering drives assortativity and community structure in ensembles of networks," *Phys. Rev. E*, vol. 84, no. 6, p. 066117, 2011.

[18] D. J. Watts and S. H. Strogatz, "Collective dynamics of small-world networks," *Nature*, vol. 393, no. 6684, pp. 440–442, 1998.

[19] D. M. Green and I. Z. Kiss, "Large-scale properties of clustered networks: Implications for disease dynamics," *J. Biol. Dyn.*, vol. 4, no. 5, pp. 431–445, 2010.

[20] M. Ritchie, L. Berthouze, T. House, and I. Z. Kiss, "Higher-order structure and epidemic dynamics in clustered networks," *J. Theor. Biol.*, vol. 348, pp. 21–32, 2014.

[21] J. C. Miller, "Percolation and epidemics in random clustered networks," *Phys. Rev. E*, vol. 80, no. 2, p. 020901, 2009.

[22] B. Karrer and M. E. J. Newman, "Random graphs containing arbitrary distributions of subgraphs," *Phys. Rev. E*, vol. 82, no. 6, p. 066118, 2010.

[23] E. M. Volz, J. C. Miller, A. Galvani, and L. A. Meyers, "Effects of heterogeneous and clustered contact patterns on infectious disease dynamics," *PLoS Comput. Biol.*, vol. 7, no. 6, p. e1002042, 2011.

[24] M. Ritchie, L. Berthouze, and I. Z. Kiss, "Beyond clustering: Mean-field dynamics on networks with arbitrary subgraph composition," *J. Mat. Biol.*, vol. 72, no. 1, pp. 255–281, 2015.

[25] K. Gough, "The estimation of latent and infectious periods," *Biometrika*, vol. 64, no. 3, pp. 559–565, 1977.

[26] A. L. Lloyd, "Realistic distributions of infectious periods in epidemic models: changing patterns of persistence and dynamics," *Theor. Pop. Biol.*, vol. 60, no. 1, pp. 59–71, 2001.

[27] H. J. Wearing, P. Rohani, and M. J. Keeling, "Appropriate models for the management of infectious diseases," *PLoS Med.*, vol. 2, no. 7, p. e174, 2005.

[28] I. Z. Kiss, G. Röst, and Z. Vizi, "Generalization of pairwise models to non-Markovian epidemics on networks," *Phys. Rev. Lett.*, vol. 115, p. 078701, 2015.

[29] G. Röst, Z. Vizi, and I. Kiss, "Pairwise approximation for SIR type network epidemics with non-Markovian recovery," *arXiv preprint arXiv:1605.02933*, 2016.

[30] B. Karrer and M. E. J. Newman, "Message passing approach for general epidemic models," *Phys. Rev. E*, vol. 82, no. 1, p. 016101, 2010.

[31] R. R. Wilkinson and K. J. Sharkey, "Message passing and moment closure for susceptible-infected-recovered epidemics on finite networks," *Phys. Rev. E*, vol. 89, no. 2, p. 022808, 2014.

[32] E. Cator, R. Van de Bovenkamp, and P. Van Mieghem, "Susceptible-infected-susceptible epidemics on networks with general infection and cure times," *Phys. Rev. E*, vol. 87, no. 6, p. 062816, 2013.

[33] N. Sherborne, K. B. Blyuss, and I. Z. Kiss, "Dynamics of multi-stage infections on networks," *Bull. Math. Biol.*, vol. 77, no. 10, pp. 1909–1933, 2015.

[34] P. L. Simon and I. Z. Kiss, "Super compact pairwise model for SIS epidemic on heterogeneous networks," *J. Comp. Net.*, 2015.

[35] R. Durrett, *Probability: Theory and Examples*. CUP, Cambridge, 2010.

[36] T. House and M. J. Keeling, "Insights from unifying modern approximations to infections on networks," *J. R. Soc. Interface*, vol. 8, no. 54, pp. 67–73, 2011.

[37] M. J. Keeling and B. Grenfell, "Disease extinction and community size: modeling the persistence of measles," *Science*, vol. 275, no. 5296, pp. 65–67, 1997.

[38] K. T. Eames and M. J. Keeling, "Modeling dynamic and network heterogeneities in the spread of sexually transmitted diseases," *Proc. Nat. Acad. Sci.*, vol. 99, no. 20, pp. 13330–13335, 2002.

[39] M. S. Shkarayev, I. Tunc, and L. B. Shaw, "Epidemics with temporary link deactivation in scale-free networks," *J. Phys. A*, vol. 47, no. 45, p. 455006, 2014.

[40] E. A. Bender and E. R. Canfield, "The asymptotic number of labeled graphs with given degree sequences," *J. Comb. Theory A*, vol. 24, no. 3, pp. 296–307, 1978.

[41] L. Pellis, S. E. F. Spencer, and T. House, "Real-time growth rate for general stochastic SIR epidemics on unclustered networks," *Math. Biosci.*, vol. 265, pp. 65–81, 2015.

[42] C. Kamp, M. Moslonka-Lefebvre, and S. Alizon, "Epidemic spread on weighted networks," *PLoS Comput. Biol.*, vol. 9, no. 12, p. e1003352, 2013.

[43] O. Diekmann, M. De Jong, and J. A. J. Metz, "A deterministic epidemic model taking account of repeated contacts between the same individuals," *J. Appl. Prob.*, vol. 35, pp. 448–462, 1998.

[44] M. E. J. Newman, "Spread of epidemic disease on networks," *Phys. Rev. E*, vol. 66, no. 1, p. 016128, 2002.

[45] E. Kenah and J. M. Robins, "Second look at the spread of epidemics on networks," *Phys. Rev. E*, vol. 76, no. 3, p. 036113, 2007.

[46] T. House and M. J. Keeling, "Epidemic prediction and control in clustered populations," *J. Theor. Biol.*, vol. 272, no. 1, pp. 1–7, 2011.

[47] J. W. Grossman, "The evolution of the mathematical research collaboration graph," *Congressus Numerantium*, pp. 201–212, 2002.

[48] M. E. J. Newman, "The structure of scientific collaboration networks," *Proc. Natl. Acad. Sci. USA*, vol. 98, no. 2, pp. 404–409, 2001.

[49] M. E. J. Newman, "Mixing patterns in networks," *Phys. Rev. E*, vol. 67, no. 2, p. 026126, 2003.

[50] S. Bansal, S. Khandelwal, and L. A. Meyers, "Exploring biological network structure with clustered random networks," *BMC Bioinformatics*, vol. 10, no. 1, p. 405, 2009.

[51] M. E. J. Newman, "Random graphs with clustering," *Phys. Rev. Lett.*, vol. 103, no. 5, p. 058701, 2009.

[52] T. House, "Generalized network clustering and its dynamical implications," *Adv. Complex Syst.*, vol. 13, no. 03, pp. 281–291, 2010.

[53] M. Ritchie, L. Berthouze, and I. Z. Kiss, "Generation and analysis of networks with a prescribed degree sequence and subgraph family: Higher-order structure matters, in press," *J. Comp. Net*, 2016.

[54] M. E. J. Newman, "Properties of highly clustered networks," *Phys. Rev. E*, vol. 68, no. 2, p. 026121, 2003.

[55] E. M. Volz, "Random networks with tunable degree distribution and clustering," *Phys. Rev. E*, vol. 70, no. 5, p. 056115, 2004.

[56] J. P. Bagrow and D. Brockmann, "Natural emergence of clusters and bursts in network evolution," *Phys. Rev. X*, vol. 3, no. 2, p. 021016, 2013.

[57] M. E. J. Newman, "Assortative mixing in networks," *Phys. Rev. Lett*, vol. 89, no. 20, p. 208701, 2002.

[58] L. Pellis, T. House, and M. J. Keeling, "Exact and approximate moment closures for non-Markovian network epidemics," *J. Theor. Biol.*, vol. 382, pp. 160–177, 2015.

[59] K. T. Eames, "Modelling disease spread through random and regular contacts in clustered populations," *Theor. Pop. Biol.*, vol. 73, no. 1, pp. 104–111, 2008.

[60] M. Á. Serrano and M. Boguñá, "Percolation and epidemic thresholds in clustered networks," *Phys. Rev. Lett.*, vol. 97, no. 8, p. 088701, 2006.

[61] A. Chaintreau, P. Hui, J. Crowcroft, C. Diot, R. Gass, and J. Scott, "Impact of human mobility on opportunistic forwarding algorithms," *IEEE Trans. Mob. Comp.*, vol. 6, no. 6, pp. 606–620, 2007.

[62] C. Cattuto, W. Van den Broeck, A. Barrat, V. Colizza, J.-F. Pinton, and A. Vespignani, "Dynamics of person-to-person interactions from distributed RFID sensor networks," *PloS ONE*, vol. 5, no. 7, p. e11596, 2010.

[63] T. Gross, C. J. D. D'Lima, and B. Blasius, "Epidemic dynamics on an adaptive network," *Phys. Rev. Lett.*, vol. 96, p. 208701, 2006.

[64] S. Risau-Gusmán and D. H. Zanette, "Contact switching as a control strategy for epidemic outbreaks," *J. Theor. Biol.*, vol. 257, no. 1, pp. 52–60, 2009.

[65] I. Z. Kiss, L. Berthouze, T. J. Taylor, and P. L. Simon, "Modelling approaches for simple dynamic networks and applications to disease transmission models," *Proc. R. Soc. A*, vol. 468, no. 2141, pp. 1332–1355, 2012.

[66] F. Sélley, Á. Besenyei, I. Z. Kiss, and P. L. Simon, "Dynamic control of modern, network-based epidemic models," *SIAM J. Appl. Dyn. Syst.*, vol. 14, no. 1, pp. 168–187, 2015.